Improved Pellet Charge Exchange Measurements in Large Helical Device*)

Tetsuo OZAKI, Naoki TAMURA, Tetsuo SEKI, Hiroshi KASAHARA, Shigeru SUDO, Pavel GONCHAROV[1)], High-Energy Particle Group, ICH Group and LHD Experimental Group

National Institute for Fusion Science, 322-6 Oroshi, Toki, Gifu 509-5292, Japan

[1)]*Department of Plasma Physics, Saint Petersburg State Polytechnic University, 29 Polytechnicheskaya Street, 195251, Russia*

(Received 30 November 2011 / Accepted 2 August 2012)

The pellet charge exchange technique (PCX), which is a combination of the compact neutral particle analyzer and an impurity pellet, is a unique method to observe the radial energetic particle distribution. There are not only charge exchange reactions between the hydrogen in the pellet and a proton, but also between the partially ionized carbon in the pellet and the proton. The neutralization factor from energetic ion to neutral particle could be deduced from the electron temperature and the electron density of the pellet cloud. The radial profiles of energetic particle distribution were measured and compared in various ion cyclotron resonance heating (ICH) plasmas. The energetic particle flux significantly increased at the resonance layer created by the ICH. PCX provides more precise information about the resonance layer than conventional neutral particle diagnostics.

Keywords: PCX, LHD, TESPEL, pellet cloud, ICH, resonance layer, energetic particle, second harmonics

DOI: 10.1585/pfr.7.2402138

1. Introduction

In magnetic confinement fusion, the plasma fuel is auxiliarily heated by neutral beam injection (NBI), ion cyclotron resonance heating (ICH), etc. until ignition occurs. After ignition, alpha particles, which are produced by the DT reaction, heat the plasma continuously. One of the most important issues is the confinement of the energetic particles, which are produced by heating. Particle orbits in a helical device are more complicated than those in a tokamak devices because there is a helical ripple in addition to a toroidal ripple. The particle orbits in helical devices have been estimated indirectly in experiments although they are well known from computer simulation [1]. It is important to investigate the position or the energy spectrum where the heating occurs. Efficient plasma heating by ICH can be expected if we know the position of the resonance layer of the ICH and the energy spectrum at this position experimentally. To study the spectra in various plasma conditions is very important. Until now, we have had only passive charge exchange neutral particle analyzers, which can observe the particle orbit indirectly [2–4]. They are not accurate for measuring the particle orbit due to the line integration. In the Large Helical Device (LHD) [5], the measurement of local energetic particle spectra by collective Thomson scattering has started recently [6]. However it is not a standard technique for the radial profile of energetic particles for the present. The pellet charge exchange (PCX) is a unique method to directly measure the radial spectrum of high-energy particles.

2. Pellet Charge Exchange

PCX had been intensively tried to measure the alpha particles from the DT plasma in TFTR [7]. In the LHD, TESPEL (tracer encapsulated pellet) [8] has been developed mainly for measuring impurity transport. At the PCX, a polystyrene pellet of 0.9 mmϕ is injected to the plasma with a velocity of 400-500 m/s by the same injector as TESPEL [9]. The energetic neutral particles, which are produced by the charge exchange reaction between protons (or helium ions) and the pellet ablation cloud, emit to the out of plasma. The charge exchanged neutral particles are measured by the compact neutral particle analyzer (CNPA) [10] from just behind the pellet trajectory. When the measurement has been performed with sufficient time resolution (typically 0.1 ms, then the spatial resolution is 4-5 cm), the time corresponds to the position where the charge exchange occurs. Therefore the radial profile of the energetic particle spectrum can be obtained. The TESPEL injector, relevant diagnostics, measurement tools in the LHD and the principle of the PCX are mentioned elsewhere [11–13].

To obtain the accurate energetic particle distribution function, three subjects should be considered. The first one is the energy dependence of the neutralization factor in the pellet cloud. The flux of the charge exchanged neutral particles is proportional to the neutralization factor. The

author's e-mail: ozaki@nifs.ac.jp

*) This article is based on the presentation at the 21st International Toki Conference (ITC21).

charge exchange occurs not only between the protons and the hydrogen neutrals in the pellet cloud, but between the protons and the partially ionized ions (carbon ions). The charge exchange cross section between proton and carbon is less than half of that between proton and hydrogen. The charge exchange cross section between the protons and the ions has been calculated by Tolstikhina [14]. The neutralization factor has also been introduced by Goncharov [10]. The neutralization factor depends on the ion charge state distribution. To obtain the ion charge state distribution, the electron temperature and electron density of the pellet cloud are required. The electron temperature and density dependence of the ion charge state distribution is shown in Fig. 1. In this calculation, The ADAS database was used [15]. The temperature and density of the pellet cloud has been measured to be 5 eV and 7.1×10^{16} cm^{-3} by Tamura and Miroshnikov [11]. The typical diameter of the pellet cloud is about 1 cm. Here we assume the uniform density and temperature of the pellet cloud. Therefore C^{+2}:C^{+3} was assumed to be 50%:50%. Finally the accurate energy dependence of the neutralization factor could be obtained.

The second subject is the attenuation of the charge exchanged neutral particles. The attenuation strongly depends on the plasma density and $Z_{\rm eff}$. The typical value of the attenuation factor was one-tenth at the proton energy of 10 keV [10].

The third subject is the pitch angle distribution of the energetic particle. The observed spectrum is a reflection of the real distribution function in the cases of perpendicular NBI or ICH heatings because the CNPA is positioned perpendicularly to the plasma. However only the particles scattered to the CNPA direction can be detected on the tangential NBI. Therefore a correction for the non-uniformity of the distribution function is necessary.

As the pellet cloud temperature and density, and the bulk plasma parameters are known, we can obtain the neutralization factor and the attenuation factor from Fig. 1 and

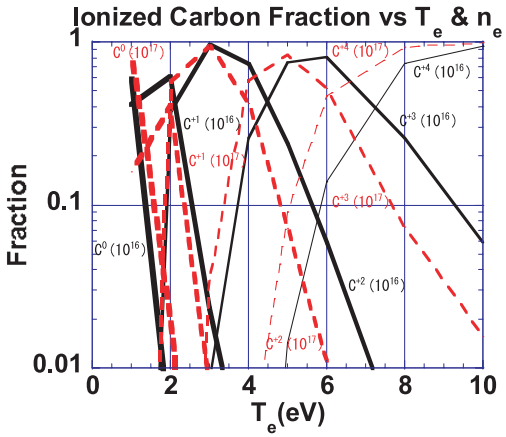

Fig. 1 Carbon ion charge state distribution The carbon ion charge state distribution depends on $T_{\rm e}$ and $n_{\rm e}$ of the pellet cloud.

the reference [10]. Here the scattering correction can be ignored because the ICH plasma will be analyzed. To simplify, a total correction factor, G, including the neutralization and attenuation factors is approximated as follows;

$$G = C_1 + C_2\rho + C_3\rho^2 + (C_4 + C_5\rho + C_6\rho^2)\log_{10}(E), \quad (1)$$

where ρ, E and C_i are the normalized minor radius, the proton energy in keV and the values determined by the plasma parameters, respectively. Typical values of C_{1-6} are −0.35, −0.68. 1.94, 0.40, 0.52 and −0.86 at the plasma density of 3.8×10^{19} m^{-3}. The accurate energy distribution function can be obtained by dividing the observed flux by G. Here the radial energy spectra of the energetic particles can be obtained by using the above correction, especially in ICH plasmas in order to investigate the heating mechanism of the ICH.

3. Radial Energetic Particle Spectra in ICH Plasmas

In the unbalanced injection of tangential NBI, the pellet trajectory is bended by the non-uniform ablation of the pellet and the trajectory comes off from the sight line of the CNPA (the sight angle of 0.8 degrees). However the radial measurement by CNPA, which is installed perpendicular against the plasma, is convenient because the direction of the particle acceleration by the ICH is also almost perpendicular to the plasma. PCX is the most suitable tool for obtaining the radial profile in the ICH plasmas.

ICH antennas are installed at ports of 3.5 U/L, 7.5 U/L. A detailed configuration of the ICH system is mentioned elsewhere [16]. The experimental conditions (the magnetic axis, the magnetic strength, heating frequency) are listed in Table 1.

3.1 Fundamental at 38.47 MHz

The ICH with the fundamental wave at the frequency of 38.47 MHz is suitable for minority ion heating. Low ICH power of 350 kW was only applied from the antenna of 3.5 U/L. In order to search the best configuration of the resonance between the ICH and the plasma, three different magnetic fields were chosen. The cases I, II and III were the resonance layers on the plasma center (2.5 T, on-axis),

Table 1 Plasma conditions in ICH experiments.

Sec.	Freq.(Hz)	$R_{\rm ax}$(m)	$B_{\rm t}$(T)	NBI
3.1(I)	38.47	3.6	2.5	N/A
(II)			2.625	N/A
(III)			2.75	N/A
3.2	38.47	3.6	1.375	#4(perp.)
3.3	51	3.75	-1.7422	#1(tang.),#4(perp.)
		3.53	-1.856	#1(tang.),#4(perp.)
3.4	38.47+85	3.6	2.75	#3(tang.)
3.5	28	3.6	2.75	N/A

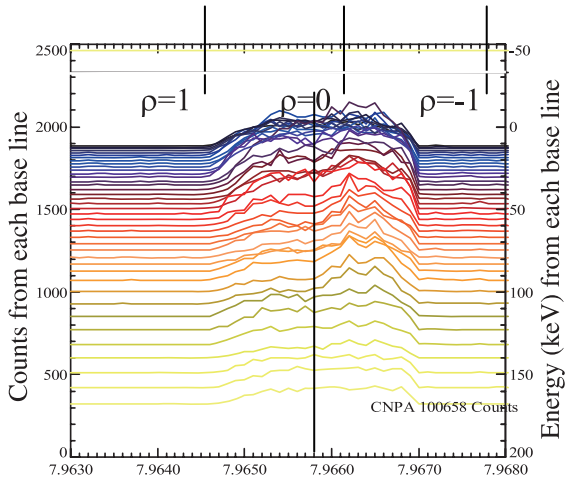

Fig. 2 PCX raw signal on second harmonics at 2.65 T. 7.9646 and 7.9678 s correspond $\rho = 1$ and -1.

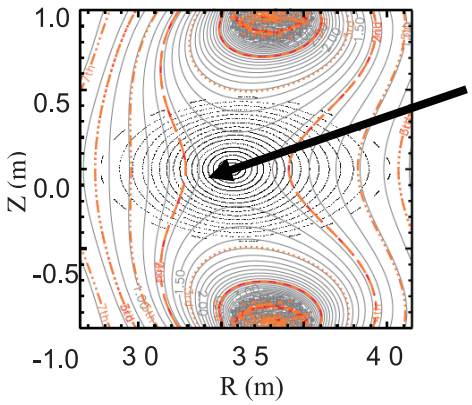

Fig. 3 Resonance layers at 1.375 T and 38.47 MHz.

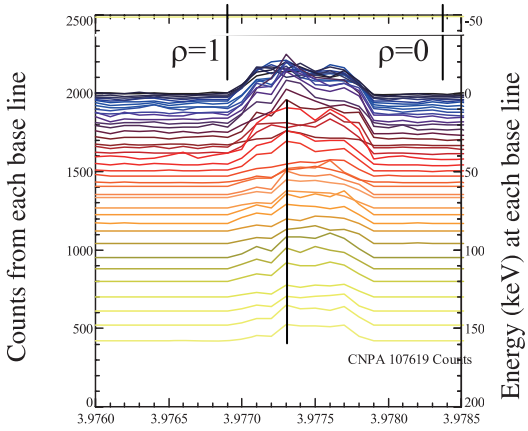

Fig. 4 PCX raw signal on second harmonics at 38.47 MHz. TESPEL passed the resonance layer at 3.9769 s.

near the plasma center (2.65 T, off-axis) and far from the plasma center (2.75 T), respectively. TESPEL reached the plasma center because the plasma density was low and the heating was only by ICH. At 2.65 T, there was no resonance layer at the low magnetic field side on the TESPEL trajectory, but there was a wide resonance layer at the high magnetic field side. As shown in Fig. 2, the particle acceleration over 50 keV could not be observed at the low magnetic field side, but widely appeared at the high magnetic field side. In the comparison between the different resonance configurations, much flux of the high-energy tail could be obtained when the resonance layer was at the plasma center (2.5 T). The result did not correspond with the results from the passive charge exchange neutral particle measurement (conventional mode of CNPA). The stored energy off-axis heating was somewhat higher than that of the off-axis heating. The analysis of this discrepancy is a future subject.

3.2 Second harmonics at 38.47 MHz

A second harmonic heating at the frequency of 38.47 MHz selectively accelerates the proton in the helium gas containing a small amount of hydrogen gas. Generally the higher harmonic heating is used in the high density and high temperature plasma. Here we verified whether it was available in LHD even if the plasma density was low. Second harmonic heating at 38.47 MHz was realized at the magnetic field of 1.375 T. The perpendicular NBI was applied at the same time because particles with high pitch angle could be easily coupled with the cyclotron resonance in ICH. Figure 3 shows the calculated resonance region on the plasma cross section. In this configuration, the resonance layer was slightly far from the plasma center (off-axis). The trajectory of TESPEL in Fig. 3 turned 20-degrees from the horizontal axis because TESPEL was injected towards the torus center on the equatorial plane from the position of 4 degrees rotated toroidaly. Figure 4 shows the time history of each energy flux. The time corresponds to the position of the TESPEL. The peak of the flux could be found near $\rho = 0.7$, where the particle acceleration occured. The width of the resonance layer is several times the Lamor radius and seems to become wider as the energy becomes lower. When the plasma density increased, the accelerated energy seemed to be low. However any change of the flux in the low energy range could not be observed by the passive charge exchange measurement.

3.3 Second harmonics at 51 MHz

Second harmonics heating has been performed at 51 MHz. By tuning the magnetic field, the same configuration of the resonance layer can be obtained as at 38.47 MHz. Due to higher magnetic field, slightly higher performance plasma can be expected. The particle acceleration of the beam from the NBI could be observed when the perpendicular NBI was injected. The particle acceleration around the resonance layer could be clearly observed in the PCX although it could not be found by the passive method. When the magnetic axis is moved inward to 3.53 m, good particle confinement should be expected because usually the trapped particles are well confined at

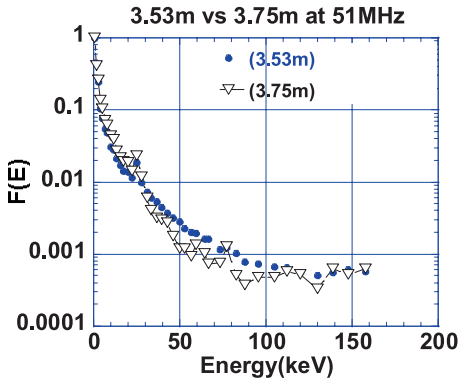

Fig. 5 Comparison of normalized energy spectra near the resonance layer at 3.75 m and 3.53 m for 51 MHz measured by PCX.

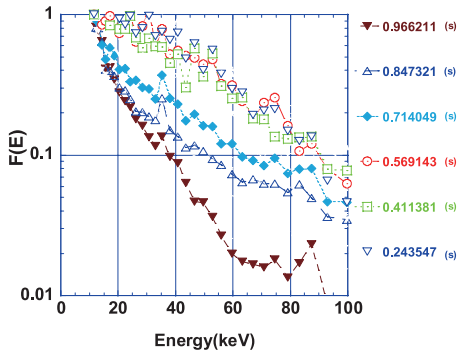

Fig. 6 Normalized energy spectrum history for 85 MHz. The high-energy tail can be observed by ICH at 85 MHz measured by PCX. At 38.47 MHz only, the spectrum did not changed from it at 0.9662 (s).

the inner magnetic axis shift. Indeed the high-energy tail could be observed by PCX at the magnetic axis position of 3.53 m rather than at 3.75 m although the particle acceleration between 20 and 60 keV was larger at 3.75 m as shown in Fig. 5. However the high-energy tail at 3.75 m seems to decrease in the passive measurement. Usually the passing particle passes near the region where the background neutral is rich at the outer magnetic axis position. The passive measurement is line integration. Therefore the particle acceleration by ICH was not clear because the passive measurement was line integrated.

3.4 Second harmonics at 85 MHz

We can perform second harmonic heating at the magnetic field of 2.75 T by using ICH at the frequency of 85 MHz. Here ICH with 85 MHz was overlapped on the plasma with ICH at 38.47 MHz (fundamental heating) and unbalanced tangential NBI. As shown in Fig. 6, the particles over 20 keV could be accelerated by the addition to the ICH with 85 MHz although the particle acceleration was not enough only by ICH with 38.47 MHz. Those energetic particles, which came from the tangential NBI might be mainly accelerated in this experiment. ICH with 85 MHz seems to be effective in LHD. In the passive measurement, a clear discrepancy could not be found although small particle acceleration around 150 keV may be observed.

3.5 Ion Bernstein Wave at 28 MHz

PCX signal can be obtained for the ion Bernstein wave (IBW) heating [17] with the frequency of 28 MHz. The magnetic axis position and magnetic field were 3.6 m and 2.75 T, respectively. The IBW heats the electron of the plasma rather than the ion. IBW may be useful to prevent sparking induced by the interaction between the plasma wall component and the accelerated ions. In calculation, the resonance layer in the IBW heating is localized near the outer region of the plasma. In the PCX, the particle acceleration could be observed only near the outer region.

4. Summary

Radial energy spectra have been observed by using PCX on ICH heating plasmas in LHD. Accurate spectra can be obtained by using the neutralization factor calculated from the temperature and density of the pellet cloud. PCX signals increased around the resonance layers in ICH plasmas. The width of the resonance layer was several times the Larmor radius. The tendency obtained by the PCX did not always correspond to that of the passive measurement due to line integration. PCX is a proper tool to observe local information of ion acceleration in ICH plasma.

Acknowledgements

The authors would like to thank Dr. Murakami who assisted with the calculation of the carbon charge state distribution. This work is financially supported by budgets NIFS10ULHH024 and NIFS10ULHH025.

[1] H. Sanuki *et al.*, Phys. Fluids B **2**, 2155 (1990).
[2] M. Isobe *et al.*, Rev. Sci. Instrum. **72**, 611 (2001).
[3] M. Osakabe *et al.*, Rev. Sci. Instrum. **75**, 3601 (2004).
[4] M. Sasao *et al.*, J. Nucl. Mater. **313-316**, 1010 (2003).
[5] O. Motojima *et al.*, Fusion Eng. Des. **20**, 3 (1993).
[6] S. Kubo *et al.*, Plasma Fusion Res. **5**, S2103 (2010).
[7] R Fisher *et al.*, Phys. Rev. Lett. **75**, 846 (1995).
[8] S. Sudo *et al.*, Rev. Sci. Instrum. **83**, 023503 (2012).
[9] P. Goncharov *et al.*, Rev. Sci. Instrum. **74**, 1869 (2003).
[10] P. Goncharov *et al.*, Rev. Sci. Instrum. **79**, 10F312 (2008).
[11] N. Tamura *et al.*, Rev. Sci. Instrum. **79**, 10F541 (2008).
[12] I. Yamada *et al.*, Rev. Sci. Instrum. **81**, 10D522 (2010).
[13] S. Sakakibara *et al.*, Fusion Eng. Des. **34-35**, 707 (1997).
[14] I. Tortihina *et al.*, private communication.
[15] H. Summers, ADAS User Manual, ver. 2.6. (2004).
[16] T. Mutoh *et al.*, Plasma Phys. Control. Fusion **42**, Issue 3, 265 (2000).
[17] R. Kumazawa *et al.*, Fusion Eng. Des. **26**, Issue 1-4, 395 (1995).